Spin-Labeled Pyridines IX-XI. In these ligands the metal-nitroxyl linkage is via the 2-carbon of the nitroxyl ring, instead of the 3-carbon. The values of *J* for the complexes of IX were similar to those for complexes of VIII. In IX there is a saturated $(CH_2)_2$ linkage between the 4-position of the pyridine and the 2-carbon of a saturated five-membered-ring nitroxyl. In VIII there is an unsaturated $(CH)_2$ linkage between the 4-position of the pyridine and the 3-carbon of an unsaturated five-membered-ring nitroxyl, which makes the metal-nitroxyl linkage one carbon longer for VIII than for IX. The similarity in the values of *J* for the complexes of VIII and IX indicates that the nature of the bonding in the metal-nitroxyl linkage is more important than the number of atoms in the linkage—the longer unsaturated linkage is as effective in spin delocalization as the shorter saturated linkage.

The values of *J* for the complexes of ligands X and XI with $Cu(hfac)_2$, Co(P), and $VO(hfac)_2$ were so large that the metal and nitroxyl inner lines occurred at the average of the metal and nitroxyl *g* values. As a result, only a lower limit could be placed on the value of *J*.

Conclusion

The values of *J* for the isoquinoline complexes were about a factor of 10 smaller than for analogous pyridine derivatives due to decreases in both the σ and π contributions to the interaction. The barrier to rotation about one or more of the single bonds in the pyridine-nitroxyl linkages in III, IV, VI, and VII is about 5 kcal/mol. The differences in the value of *J* for isomers of the same ligand indicated that the value of *J* is strongly dependent on the conformation of the metal-nitroxyl linkage. *J* is about 1 order of magnitude larger for an olefinic linkage than for an amide linkage. Addition of a carbonyl group to the olefinic linkage between the pyridine and the nitroxyl caused a smaller decrease in the value of *J* when the carbonyl group was adjacent to the pyridine ring (factor of 9-18) than when it was adjacent to the nitroxyl ring (factor of 23-72). When the position of the substituent on the pyridine ring was varied and the 2-isomer could not form a chelate ring, the values of *J* decreased in the order 2-isomer > 4-isomer > 3-isomer for Cu(II), 4-isomer $\approx$ 3-isomer for Co(II), and 4-isomer > 3-isomer for vanadyl.

Acknowledgment. The partial support of this work by NIH Grant GM21156 (G.R.E. and S.S.E.) and by Grant 301/A/82 from the Hungarian Scientific Academy (K.H. and O.H.H.) is gratefully acknowledged. Purchase of the IBM ER200 spectrometer was funded in part by NSF Grant CHE8411282 (G.R.E. and S.S.E.). We are grateful to Professor P. Sohár (Budapest, Hungary) for running NMR spectra.

Contribution from the Biomedical Chemistry Research Center,
Department of Chemistry, University of Cincinnati, Cincinnati, Ohio 45221-0172

Synthesis and Characterization of Technetium(III) Complexes Containing 2,2′-Bipyridine and 1,10-Phenanthroline. X-ray Crystal Structures of *cis*(*Cl*),*trans*(*P*)-$[TcCl_2(P(CH_3)_2C_6H_5)_2(bpy)]B(C_6H_5)_4$, *cis*(*Cl*),*trans*(*P*)-$[TcCl_2(P(CH_3)_2C_6H_5)_2(phen)]B(C_6H_5)_4$, and *cis*(*Cl*),*trans*(*P*)-$[TcCl_2(P(CH_3CH_2)(C_6H_5)_2)_2(bpy)]SO_3CF_3$[1]

Bruce E. Wilcox,[2] Douglas M. Ho, and Edward Deutsch*

Received August 19, 1988

Technetium(III) complexes of the general formula *cis*(*Cl*),*trans*(*P*)-$[TcCl_2(P)_2L]^+$, where (P) is dimethylphenylphosphine (PMe_2Ph) or ethyldiphenylphosphine ($PEtPh_2$) and L is 2,2′-bipyridine (bpy), 4,4′-dimethyl-2,2′-bipyridine (Me_2bpy), or 1,10-phenanthroline (phen), have been synthesized and characterized. They are prepared by L substitution onto, with concomitant displacement of one chloride and one phosphine ligand from, the *mer*-$TcCl_3(P)_3$ starting material in refluxing ethanol. Analysis of these complexes by fast atom bombardment mass spectrometry (in the positive ion mode) provides "fingerprint" mass spectra that exhibit peaks assigned to the molecular ion M^+ as well as peaks assigned to M^+ minus one or more monodentate ligands. Single-crystal X-ray structure determinations of *cis*(*Cl*),*trans*(*P*)-$[TcCl_2(PMe_2Ph)_2(bpy)]BPh_4$ (A), *cis*(*Cl*),*trans*(*P*)-$[TcCl_2(PMe_2Ph)_2(phen)]BPh_4$ (B), and *cis*(*Cl*),*trans*(*P*)-$[TcCl_2(PEtPh_2)_2(bpy)]SO_3CF_3$ (C), with formula weights of 921.62, 945.64, and 903.65, respectively, show that the technetium atoms reside in slightly distorted octahedral environments. Complex A crystallizes in the triclinic space group $P\bar{1}$, with $a = 10.700$ (2) Å, $b = 14.231$ (2) Å, $c = 16.018$ (2) Å, $\alpha = 95.80$ (1)°, $\beta = 97.58$ (1)°, $\gamma = 108.34$ (1)°, and $V = 2268.5$ (6) Å^3, with $Z = 2$ for 3104 observed reflections with $F > 6\sigma(F)$. Complex B crystallizes in the triclinic space group $P\bar{1}$ with $a = 10.668$ (2) Å, $b = 14.064$ (2) Å, $c = 16.529$ (2) Å, $\alpha = 95.50$ (1)°, $\beta = 97.61$ (1)°, $\gamma = 108.67$ (1)°, and $V = 2309.3$ (7) Å^3, with $Z = 2$ for 4975 observed reflections with $F > 3\sigma(F)$. Complex C crystallizes in the orthorhombic space group $P2_12_12_1$ with $a = 16.399$ (2) Å, $b = 21.869$ (5) Å, $c = 11.102$ (2) Å, and $V = 3982$ (1) Å^3, with $Z = 4$ for 3585 observed reflections with $F > 6\sigma(F)$.

Introduction

The chemistry and physical properties of polypyridyl complexes containing a wide variety of transition metals have been, and are continuing to be, studied extensively.[3-5] Conspicuously ill represented in this list of metals is technetium. To date, only mono(bipyridine) or -(phenanthroline) complexes of technetium(VII) and technetium(V)[6] and mono- or bis(pyridine) complexes of technetium(IV)[7] have been reported. There are no reports of polypyridyl-technetium complexes in which the technetium center exhibits an oxidation less than +4. This is due in part to the fact that technetium chemistry has only recently begun to be developed[8]

---

[1] Abstracted from: Wilcox, B. E. Ph.D. Dissertation, University of Cincinnati, 1987.

[2] Current address: Department of Chemistry, Bloomsburg University, Bloomsburg, PA 17815.

(3) (a) Bond, A. M.; Haga, M. *Inorg. Chem.* **1986**, *25*, 4507 and references therein. (b) Ohsawa, Y.; DeArmond, M. K.; Hanck, K. W.; et al. *J. Am. Chem. Soc.* **1983**, *105*, 6522 and references therein. (c) Rillema, D. P.; Taghidiri, D. G.; Jones, D. S.; et al. *Inorg. Chem.* **1987**, *26*, 578 and references therein. (d) Stebler, M.; Ludi, A.; Bürgi, H.-B. *Inorg. Chem.* **1986**, *25*, 4743 and references therein. (e) Nord, G. *Comments Inorg. Chem.* **1985**, *74*, 193. (f) Constable, E. C. In *Advances in Inorganic Chemistry and Radiochemistry*; Emeleus, H. J., Sharpe, A. G., Eds.; 1986, Academic Press: New York, p 69.

(4) Caspar, J. V.; Sullivan, B. P.; Meyer, T. J. *Inorg. Chem.* **1984**, *23*, 2104 and references therein.

0020-1669/89/1328-1743$01.50/0 © 1989 American Chemical Society

Table I. Crystal, Data Collection, and Refinement Parameters for *cis(Cl),trans(P)*-[$TcCl_2(PMe_2Ph)_2(bpy)$]BPh_4 (A), *cis(Cl),trans(P)*-[$TcCl_2(PMe_2Ph)_2(phen)$]BPh_4 (B), and *cis(Cl),trans(P)*-[$TcCl_2(PEtPh_2)_2(bpy)$]SO_3CF_3 (C)[a]

	A	B	C
empirical formula	$C_{50}H_{50}BCl_2N_2P_2Tc$	$C_{52}H_{50}BCl_2N_2P_2Tc$	$C_{39}H_{38}Cl_2F_3N_2O_3P_2STc$
size, mm	0.22 × 0.32 × 0.32	0.32 × 0.38 × 0.38	0.12 × 0.12 × 0.55
cryst syst	triclinic	triclinic	orthorhombic
space group	$P\bar{1}$ (No. 2)	$\mathrm{P}\bar{1}$ (No. 2)	$P2_12_1i_1$ (No. 19)
a, Å	10.700 (2)	10.668 (2)	16.399 (2)
b, Å	14.231 (2)	14.064 (2)	21.869 (5)
c, Å	16.018 (2)	16.529 (2)	11.102 (2)
α, deg	95.80 (1)	95.50 (1)	90
β, deg	97.58 (1)	97.61 (1)	90
γ, deg	108.34 (1)	108.67 (1)	90
V, $Å^3$	2268.5 (6)	2309.3 (7)	3982 (1)
Z	2	2	4
fw	921.62	945.64	903.65
ρ_{calcd}, g cm^{-3}	1.35	1.36	1.51
F(000), e	952	976	1840
λ(Mo Kα), Å	0.71073	0.71073	0.71073
monochromator	highly oriented graphite crystal		
hkl limits	13,±17,±19	13,±17,±19	+19,+24,+14 and −19,−24,−14
2θ range, deg	3–45	3–45	3–45
scan type	$\theta/2\theta$	$\theta/2\theta$	$\theta/2\theta$
scan speed, deg/min	4.0–29.3	4.0–29.3	2.0–29.3
scan range, deg	0.9 below Kα_1 to 0.9 above Kα_2		0.8 below to 0.8 above
bkgd meas	stationary cryst and counter at beginning and end of scan; total bkgd time to scan time ratio of 0.5		
std reflcns	3 measd every 37 reflcns		
no. of measd reflcns	6356 (5958 indep)	6469 (6067 indep)	5972 (4919 indep)
no. of obsd reflcns	3104; $F > 3\sigma(F)$	4975; $F > 3\sigma(F)$	3585; $F > 6\sigma(F)$
abs coeff, cm^{-1}	4.94	4.88	6.26
R[b]	0.0756	0.0362	0.0470
R_w[c]	0.0808	0.0386[d,e]	0.0596[d,f]
goodness of fit (S)[g]	3.16	1.31	1.17
largest shift/esd	0.000	0.004	0.001
no. variables	524	543	481
data/param. ratio	5.9:1	9.2:1	7.5:1
$\Delta\rho_{max}$, e $Å^{-3}$	0.55	0.39	1.4

[a] Ligand abbreviations defined in the Abbreviations section. [b] $R = \sum(|F_o| - |F_c|)/\sum|F_o|$. [c] $R_w = [\sum w(|F_o| - |F_c|)^2/\sum w|F_o|^2]^{1/2}$. [d] $w = [\sigma^2(F) + |g|F^2]^{-1}$. [e] $g = 0.000262$. [f] $g = 0.001320$. [g] $S = [\sum w(|F_o| - |F_c|)^2/(M - N)]^{1/2}$, where *M* is the number of observed reflections and *N* is the number of parameters refined.

and in part to the lack of convenient starting materials that in general are available for other transition metals.[9]

Meyer and co-workers have reported on the synthesis of rhenium(III) and rhenium(I) mono(bipyridyl) complexes.[4] Since rhenium and technetium are in the same periodic group, there are similarities in their chemistries that can often guide the syntheses of congeners. Thus, the reported syntheses of low-valent rhenium–bipyridine complexes have facilitated the preparation of low-valent technetium–polypyridyl complexes reported herein.

Abbreviations

bpy = 2,2′-bipyridine

phen = 1,10-phenanthroline

Me_2bpy = 4,4′-dimethyl-2,2′-bipyridine

PMe_2Ph = dimethylphenylphosphine

$PEtPh_2$ = ethyldiphenylphosphine

DPPE = $Ph_2PCH_2CH_2PPh_2$

DMPE = $(CH_3)_2PCH_2CH_2P(CH_3)_2$

BPh_4^- = tetraphenylborate anion

$(acac)_2en^{2-}$ = $CH_3COCHC(CH_3)NCH_2CH_2NC(CH_3)CHCOCH_3^{2-}$

Ph = phenyl

Me = methyl

Et = ethyl

Experimental Section

Materials. Technetium-99 emits a low-energy (0.292 MeV) β particle with a half-life of 2.12 × 10^5 years. When this material is handled in milligram amounts, it does not present a serious health hazard since common laboratory materials provide adequate shielding. Bremsstralung is not a significant problem due to the low energy of the β-particle emission, but normal radiation safety procedures must be used at all times, especially when dealing with solid samples, to prevent contamination. All solvents and reagents used were of reagent grade. $NH_4{}^{99}TcO_4$ was obtained from Oak Ridge National Laboratory and was dissolved in water and then treated with a small amount of 30% H_2O_2 (Fisher) to oxidize any TcO_2 impurity to pertechnetate. Dimethylphenylphosphine and ethyldiphenylphosphine (Strem Chemicals), 2,2′-bipyridine (Aldrich), 4,4′-dimethyl-2,2′-bipyridine, and 1,10-phenanthroline (GFS Chemicals) were used as received. The technetium(III) starting materials *mer*-$TcCl_3(PMe_2Ph)_3$, *mer*-$TcBr_3(PMe_2Ph)_3$, and *mer*-$TcCl_3(PEtPh_2)_3$ were prepared as previously reported.[10] Chromatographic separations were performed on Sephadex LH-20 lipophilic resin (Pharmacia).

Physical Measurements. UV–visible spectra were recorded on a Cary 210 spectrophotometer (Varian Instruments) in acetonitrile solutions. Mass spectra were recorded on a VG 30-250 quadrupole mass spectrometer (VG Masslab) with a fast atom bombardment (FAB) ionization source using xenon as the bombardment gas. Samples from mass analysis were prepared by dissolving or suspending solid samples in one of the following matrices: glycerol (Fisher), "Magic Matrix" (5:1 dithio-

---

(5) Stebler, M.; Gutierrez, A.; Ludi, A.; Bürgi, H.-B. *Inorg. Chem.* **1987**, *26*, 1449 and references therein.

(6) Davison, A.; Jones, A. G.; Abrams, M. J. *Inorg. Chem.* **1981**, *20*, 4300.

(7) Fergusson, J. E.; Hickford, J. H. *J. Inorg.* Nucl. *Chem.* **1966**, *28*, 2293.

(8) Deutsch, E.; Libson, K.; Jurisson, S.; Lindoy, L. F. In *Progress in Inorganic Chemistry*; Lippard, S. J., Ed.; John Wiley and Sons: New York, 1983; Vol. 30.

(9) Cotton, F. A. and Wilkinson, G. *Advanced Inorganic Chemistry*, 4th ed.; Interscience: New York, 1980.

(10) Mazzi, U.; DePaoli, G.; DiBernardo, P.; Magon, L. *J. Inorg. Nucl. Chem.* **1976**, *38*, 721.

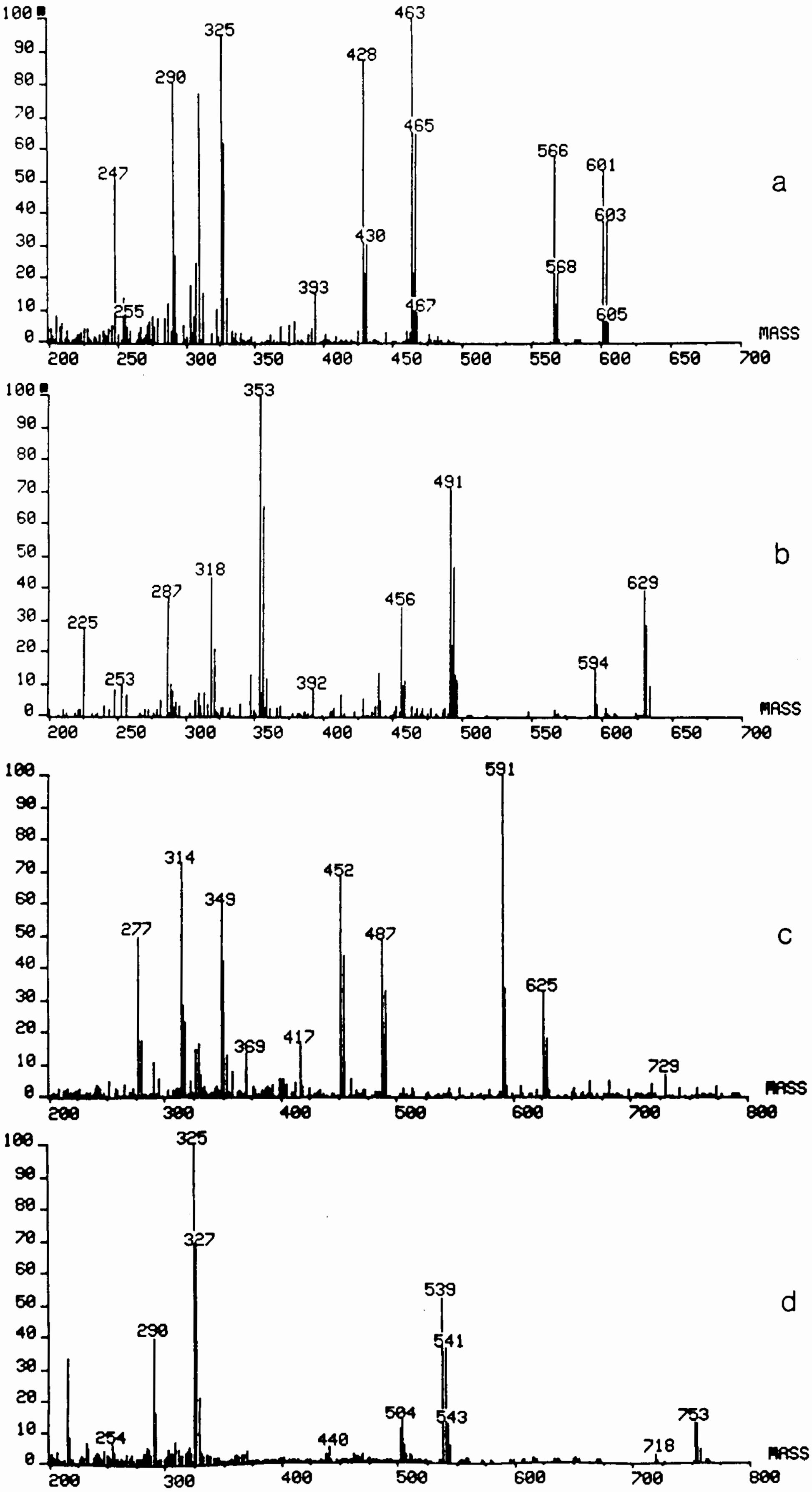

Figure 1. Fast atom bombardment mass spectra of (a) *cis*(*Cl*),*trans*(*P*)-$[TcCl_2(PMe_2Ph)_2(bpy)]^+$, (b) *cis*(*Cl*),*trans*(*P*)-$[TcCl_2(PMe_2Ph)_2(Me_2bpy)]^+$, (c) *cis*(*Cl*),*trans*(*P*)-$[TcCl_2(PMe_2Ph)_2(phen)]^+$, and (d) *cis*(*Cl*),*trans*(*P*)-$[TcCl_2(PEtPh_2)_2(bpy)]^+$, showing fragmentation patterns indicative of the loss of monodentate ligands from the complex ion.

threitol–dithioerythritol (Sigma Chemicals) with a small amount of methanol), or *m*-nitrobenzyl alcohol (Kodak). For mass analysis of chromatographic bands, portions of the isolated fractions were allowed to evaporate to dryness in the depression of a spot plate and then were

Table II. UV-Visible Spectrophotometric Parameters of Technetium(III) Bipyridine and Phenanthroline Complexes of the Form *cis*(*X*),*trans*(*P*)-$[TcX_2(PR_2R')_2L]^{+}$ [a]

complex	λ_{max}, nm (ϵ, M^{-1} cm^{-1})
cis(*Cl*),*trans*(*P*)-$[TcCl_2(PMe_2Ph)_2(bpy)]^+$	262 (30 700), 298 (15 400), 364 (2840), 540 (2350)
cis(*Cl*),*trans*(*P*)-$[TcCl_2(PMe_2Ph)_2(phen)]^+$	264 (48 700), 388 (3110), 538 (2860)
cis(*Cl*),*trans*(*P*)-$[TcCl_2(PMe_2Ph)_2(Me_2bpy)]^+$	262 (35 000), 295 sh (16 200), 365 sh (2970), 539 (2400)
cis(*Br*),*trans*(*P*)-$[TcBr_2(PMe_2Ph)_2(bpy)]^+$ [b]	372 (4500), 535 (3290)
cis(*Cl*),*trans*(*P*)-$[TcCl_2(PEtPh_2)_2(bpy)]^+$	276 (30 800), 360 sh, 500 sh, 537 (2140)
mer-$TcCl_3(PMe_2Ph)_3$	246 (26 600), 265 (30 000), 331 (2200), 381 (1850), 481 (980)

[a] Acetonitrile solutions. [b] Values in the visible region from a spectroelectrochemistry experiment in DMF solutions (ref 14).

mixed with matrix by using a glass pestle. For chromatographic bands that were very diffuse or contained small amounts of material, it was often necessary to allow several portions to evaporate in the same depression in order to accumulate sufficient material for analysis. Elemental analyses were performed by Galbraith Laboratories, Knoxville, TN.

Synthesis of Complexes. *cis*(*Cl*),*trans*(*P*)-$[TcCl_2(PMe_2Ph)_2(bpy)]PF_6$. A 152-mg (0.245-mmol) sample of *mer*-$TcCl_3(PMe_2Ph)_3$ was dissolved in 25 mL of ethanol. Then 190 mg (1.22 mmol) of bpy was added, and the reaction mixture was refluxed for 30 min. The resulting red/purple mixture was rotoevaporated to dryness and the residue dissolved in a small amount of dichloromethane. This solution was then loaded onto a 2 × 20 cm (i.d. × length) Sephadex LH-20 column packed in dichloromethane. Elution with dichloromethane produced four bands; a yellow band, a green band, a major red/purple band, and a brown band. The red/purple band was collected and rotoevaporated to dryness, and the residue was dissolved in a small amount of methanol. Twenty drops of 1 M NH_4PF_6 in water and a small amount of water were added to this solution, and it was left overnight. The next day 105 mg of product (0.141 mmol, 58% yield) was collected by suction filtration. Anal. Calcd for $[TcP_2N_2Cl_2C_{26}H_{30}]PF_6$: C, 41.79; H, 4.05; N, 3.75; P, 12.43; Cl, 9.49. Found: C, 42.19; H, 4.11; N, 3.73; P. 12.31; Cl, 9.33. The complex can also be precipitated as the trifluoromethane sulfonate salt by dissolving the red/purple chromatographic fraction in acetone, adding 20 drops of 1 M $NaSO_3CF_3$ in acetone and 5 mL of water, and allowing the precipitate to form. The tetraphenylborate salt was prepared by metathesis from the hexafluorophosphate salt and $NaBPh_4$ in ethanol solution.

Other Analogues. The analogues containing 1,10-phenanthroline, 4,4′-dimethyl-2,2′-bipyridine, and bpy with ethyldiphenylphosphine were prepared as above in similar yield. The *cis*(*Cl*),*trans*(*P*)-$[TcBr_2(PMe_2Ph)_2(bpy)]^+$ analogue was formed in very small yield and was not recovered as a solid product.

X-ray Crystal Structure Analyses. Crystal, data collection and refinement parameters for *cis*(*Cl*),*trans*(*P*)-$[TcCl_2(PMe_2Ph)_2(bpy)]BPh_4$ (A), *cis*(*Cl*),*trans*(*P*)-$[TcCl_2(PMe_2Ph)_2(phen)]BPh_4$ (B), and *cis*(*Cl*),*trans*(*P*)-$[TcCl_2(PEtPh_2)_2(bpy)]SO_3CF_3$ (C) are found in Table I. In each case, a crystal of suitable size and quality was mounted on a glass fiber and transferred to a Nicolet R3m four-circle diffractometer for analysis and data collection at ambient temperature. Scattering factors for Tc were taken from ref 11. All other neutral-atom scattering factors were used as stored in the SHELXTL[12] or SHELXTL PLUS[13] structure determination packages.

***cis*(*Cl*),*trans*(*P*)-$[TcCl_2(PMe_2Ph)_2(bpy)]BPh_4$.** The complex crystallizes as dark violet prisms by slow evaporation from dichloromethane/toluene. Unit cell parameters were determined from the angular settings of 15 well-centered reflections ($19° < 2\theta < 28°$). Axial photographs and a limited search through an octant of reciprocal space revealed no systematic absences and no axial symmetry, suggesting that the sample had crystallized in the triclinic space group $P1$ or $P\bar{1}$. Collected reflections were corrected for Lorentz and polarization effects. No corrections for absorption or the presence of extinction were made. Three standard reflections were monitored throughout the data collection and showed random variations in their intensities. The minimum and maximum drift corrections were 0.9645 and 1.0025, respectively, indicating only nominal variations in the sample and instrument throughout the data collection. Data reduction yielded 5958 unique reflections with $R = 0.0161$ for the averaging of equivalent reflections.

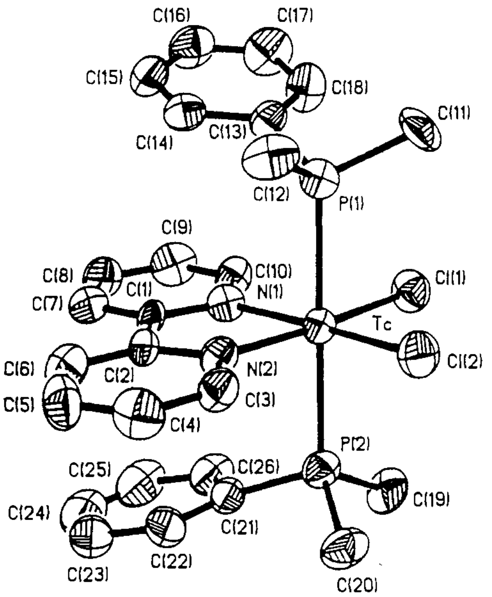

Figure 2. Molecular ion plot and atom-numbering scheme of *cis*(*Cl*),*trans*(*P*)-$[TcCl_2(PMe_2Ph)_2(bpy)]^+$.

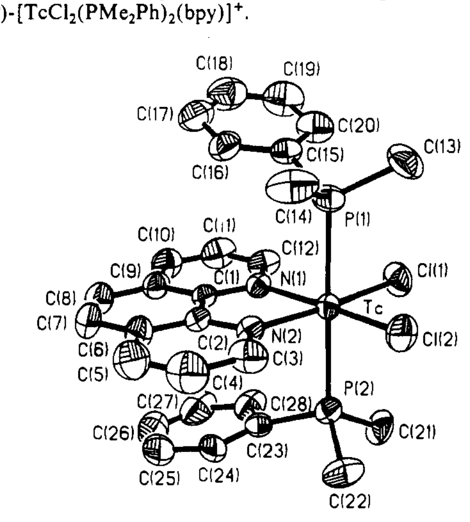

Figure 3. Molecular ion plot and atom-numbering scheme of *cis*(*Cl*),*trans*(*P*)-$[TcCl_2(PMe_2Ph)_2(phen)]^+$.

The structure was successfully solved by full-matrix least-squares methods in the triclinic space group $P\bar{1}$ (No. 2). An initial sharpened Patterson map (SHELXS with PATT option)[12] was used to derive the position of the technetium atom. Difference Fourier syntheses were used to locate the positions of the other non-hydrogen atoms. Isotropic refinement of this model with unit weights converged to $R = 0.1240$ with 3891 reflections having $F > 3\sigma(F)$. Anisotropic refinement of this model lowered the residuals to $R = 0.1051$. The inclusion of the riding model for hydrogen atoms (C–H = 0.96 Å) with isotropic temperature parameters fixed at $U(H) = 0.08$ Å^2 led to a further reduction in the residuals to $R = 0.0979$ and $R_w = 0.0971$. The final residuals were $R = 0.0756$ and $R_w = 0.0808$ with goodness-of-fit $S = 3.16$.

***cis*(*Cl*),*trans*(*P*)-$[TcCl_2(PMe_2Ph)_2(phen)]BPh_4$.** Crystals were obtained as dark purple prisms by slow evaporation from dichloromethane/toluene. The unit cell analysis and data collection were carried out as they were for the bpy analogue above with the following modifications: angular settings of 15 standard reflections ($21° < 2\theta < 29°$); minimum and maximum drift corrections, 0.9843 and 1.0124, respectively. No corrections for absorption or extinction were made. Data reduction yielded 6067 independent reflections with $R = 0.0164$ for the averaging of equivalent reflections.

The structure was successfully solved and refined by full-matrix least-squares methods in the triclinic space group $P\bar{1}$ (No. 2) as above. Isotropic refinement of this model with unit weights converged to $R =$

---

(11) *International Tables for X-Ray Crystallography*; Kynoch: Birmingham, England, 1974.

(12) All computations were made with SHELXTL (Nicolet, VMS prerelease, 1986) on a MicroVAX II computer.

(13) All computations were made with SHELXTL PLUS (Nicolet, 1986) on a MicroVAX II computer.

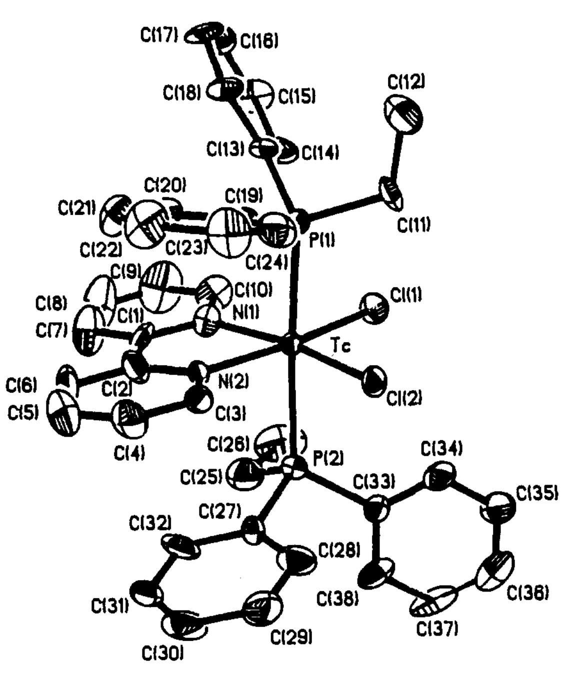

Figure 4. Molecular ion plot and atom-numbering scheme of *cis*(*Cl*),*trans*(*P*)-$[TcCl_2(PEtPh_2)_2(bpy)]^+$.

0.0818 with uncorrected data. Anisotropic refinement of this model lowered the residuals to $R = 0.0524$. Subsequent cycles of least-squares refinement included a weighting scheme based on $\sigma(F)$, and hydrogen atoms riding on their respective carbon atoms with C–H = 0.96 Å. Two common hydrogen isotropic temperature parameters [U(H) for aromatic and U(H)′ for methyl hydrogen atoms] were included and allowed to vary. This model refined smoothly to the final residuals $R = 0.0362$ and $R_w = 0.0386$ with goodness-of-fit $S = 1.31$. The refined hydrogen isotropic parameters were U(H) = 0.102 (5) Å^2, and U(H)′ = 0.074 (2) Å^2.

***cis*-(*Cl*),*trans*(*P*)-$[TcCl_2(PEtPh_2)_2(bpy)]SO_3CF_3$.** Crystals were obtained as dark red/purple prisms by slow evaporation from ethanol/water. The unit cell analysis and data collection were carried out as they were for the other analogues above with the following modifications: angular settings of 25 reflections ($19° < 2\theta < 26°$); minimum and maximum drift corrections, 0.9911 and 1.0457, respectively; minimum and maximum transmission factors, 0.302 and 0.450, respectively; revealed systematic absences and symmetry consistent with the orthorhombic space group $P2_12_12_1$ (No. 19). Empirical absorption corrections were made with SHELXTL PLUS (XEMP) based on five azimuthal reflections. No correction for the presence of extinction was made. A total of 4919 unique reflections with $R = 0.0274$ for the averaging of equivalent reflections were obtained.

The structure was successfully solved and refined by full-matrix least-squares methods. A combination of direct methods (SHELXS with TREF option)[13] and difference Fourier methods were used to locate the positions of the non-hydrogen atoms. The presence of a disordered trifluoromethanesulfonate anion was evident in the early stages of structure solution and refinement. All attempts to locate a suitably well-balanced disorder model were without success. Isotropic refinement of this model with unit weights converged to $R = 0.0718$ with uncorrected data. Anisotropic refinement of this model lowered the residuals to $R = 0.0520$. Subsequent cycles of least-squares refinement included absorption-corrected data, a weighting scheme based on $\sigma(F)$, and hydrogen atoms riding on their respective carbon atoms with C–H = 0.96 Å. Three common hydrogen isotropic temperature parameters [U(H) for aromatic, U(H)′ for methylene, and U(H)″ for methyl hydrogen atoms] were included and allowed to vary. This model refined smoothly to the final residuals $R = 0.0470$ and $R_w = 0.0596$ with goodness-of-fit being $S = 1.17$. (Refinement of the inverse structure gave $R = 0.0472$, $R_w = 0.0597$, and $S = 1.18$.) The refined hydrogen isotropic parameters were U(H) = 0.059 (7) Å^2, U(H)′ = 0.052 (18) Å^2, and U(H)″ = 0.111 (25) Å^2.

Results

Synthesis and Characterization. Technetium(III) complexes of the general formula $[TcCl_2(P)_2L]^+$, where (P) = dimethylphenylphosphine or ethyldiphenylphosphine and L = 2,2′-bipyridine, 4,4′-dimethyl-2,2′-bipyridine, or 1,10-phenanthroline, are prepared by replacement of one chloride and one phosphine ligand of the *mer*-$TcCl_3(P)_3$ starting material by the bidentate L ligand. They are isolated as trifluoromethanesulfonate, hexafluorophosphate, or tetraphenylborate salts after purification on Sephadex LH-20 lipophilic resin. They are characterized by (1) elemental analyses of the prototype complex *cis*(*Cl*),*trans*(*P*)-$[TcCl_2(PMe_2Ph)_2(bpy)]PF_6$, which give results consistent with the proposed formulation; (2) analogous UV–visible spectrophotometric parameters given in Table II; (3) fast atom bombardment mass spectra, Figure 1; and (4) the single-crystal structural analyses of *cis*(*Cl*),*trans*(*P*)-$[TcCl_2(PMe_2Ph)_2(bpy)]BPh_4$, *cis*(*Cl*),*trans*(*P*)-$[TcCl_2(PMe_2Ph)_2(phen)]BPh_4$, and *cis*(*Cl*),*trans*(*P*)-$[TcCl_2(PEtPh_2)_2(bpy)]SO_3CF_3$.

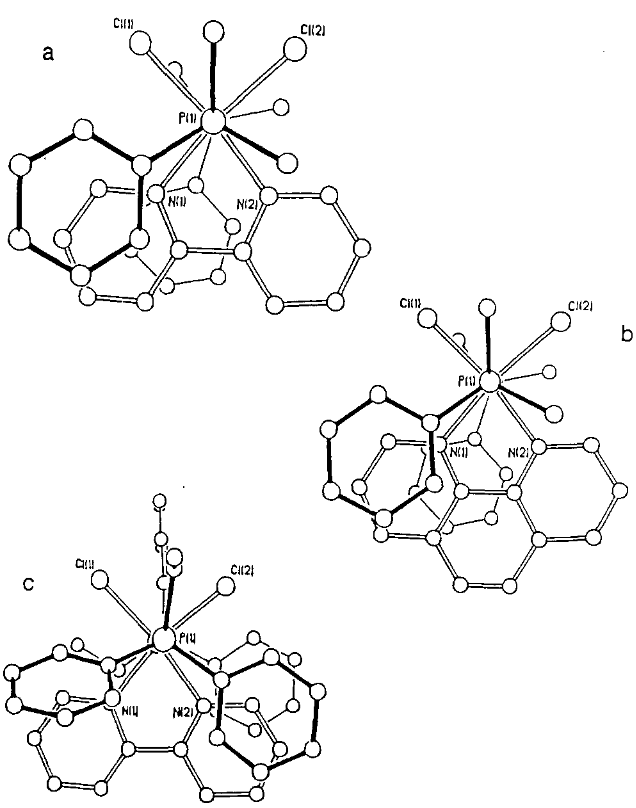

Figure 5. Molecular plots viewed down the P–Tc–P axes of (a) *cis*(*Cl*),*trans*(*P*)-$[TcCl_2(PMe_2Ph)_2(bpy)]^+$, (b) *cis*(*Cl*),*trans*(*P*)-$[TcCl_2(PMe_2Ph)_2(phen)]^+$, and (c) *cis*(*Cl*),*trans*(*P*)-$[TcCl_2(PEtPh_2)_2(bpy)]^+$.

Table II lists the UV–visible spectrophotometric parameters for the complexes, all of which exhibit strong absorbances between 300 and 600 nm and are intensely colored. All appear red to red/purple in solution. Fast atom bombardment mass spectra of the complexes are shown in Figure 1. The peak cluster of highest mass in each spectrum is assigned to the molecular ion M^+. In addition, these mass spectra exhibit extensive fragmentation patterns. Mass spectra taken of samples from chromatographic fractions other than the major product also exhibit peaks that can be assigned reasonable formulations. For example, the spectrum of the green fraction preceding the major product fraction in the chromatography of the $[TcCl_2(PMe_2Ph)_2bpy]^+$ preparation mixture exhibits a molecular ion at m/e 601 (the same as for the major red/purple product) and an identical fragmentation pattern. This product has been identified as the Tc(II) analogue of the Tc(III) parent $[TcCl_2(PMe_2Ph)_2(bpy)]^+$.[14] Also, there is evidence for the formation of a complex of the formulation $TcCl(PMe_2Ph)_3(bpy)$.

X-ray Crystal Structures. Final atomic positional parameters and equivalent isotropic displacement parameters for all non-hydrogen atoms are found in Table III. Selected bond lengths and angles for the complexes are found in Table IV. Molecular structure plots with associated atom-numbering schemes are found as follows: *cis*(*Cl*),*trans*(*P*)-$[TcCl_2(PMe_2Ph)_2(bpy)]^+$, Figure 2;

---

(14) Wilcox, B. E. Ph.D. Dissertation, University of Cincinnati, 1987.

Table III. Final Atomic Positional Parameters (×10⁴) and Equivalent Isotropic Displacement Parameters (Å² × 10³)

atom	*x*	*y*	*z*	*U*(eq)[a]	atom	*x*	*y*	*z*	*U*(eq)[a]
a. *cis*(*Cl*),*trans*(*P*)-$[\mathrm{TcCl_2(PMe_2Ph)_2(bpy)}]\mathrm{BPh_4}$									
Tc	1060 (1)	2616 (1)	4189 (1)	56 (1)	C(22)	−3069 (18)	1511 (17)	3125 (13)	98 (11)
P(1)	3257 (4)	2740 (3)	3820 (3)	70 (2)	C(23)	−3847 (22)	1459 (23)	2345 (16)	124 (15)
P(2)	−1148 (4)	2483 (3)	4578 (3)	74 (2)	C(24)	−3877 (26)	2346 (30)	2087 (19)	146 (22)
Cl(1)	2082 (4)	4197 (3)	5039 (3)	86 (2)	C(25)	−3196 (26)	3256 (25)	2559 (17)	134 (18)
Cl(2)	1518 (4)	1703 (3)	5269 (3)	85 (2)	C(26)	−2419 (19)	3305 (16)	3356 (13)	97 (11)
N(1)	594 (12)	3175 (9)	3099 (8)	61 (6)	C(27)	7381 (16)	2857 (11)	9212 (9)	65 (7)
N(2)	101 (12)	1347 (9)	3309 (8)	62 (6)	C(28)	6105 (21)	2667 (13)	9470 (13)	117 (11)
B	7708 (18)	2008 (12)	8590 (11)	62 (8)	C(29)	5762 (22)	3368 (15)	9960 (14)	120 (12)
C(1)	−86 (14)	2502 (13)	2389 (9)	61 (7)	C(30)	6639 (22)	4309 (15)	10217 (11)	93 (10)
C(2)	−366 (14)	1461 (11)	2506 (10)	60 (7)	C(31)	7848 (18)	4555 (12)	9951 (10)	79 (8)
C(3)	−164 (15)	383 (12)	3454 (10)	73 (8)	C(32)	8204 (16)	3838 (12)	9461 (10)	74 (8)
C(4)	−849 (18)	−446 (14)	2821 (14)	96 (10)	C(33)	9226 (16)	2454 (10)	8397 (10)	66 (7)
C(5)	−1290 (18)	−291 (15)	2034 (12)	98 (10)	C(34)	9546 (18)	2737 (12)	7626 (11)	88 (9)
C(6)	−1043 (17)	679 (14)	1858 (11)	87 (9)	C(35)	10848 (23)	3106 (13)	7475 (13)	97 (10)
C(7)	−454 (16)	2813 (14)	1623 (11)	85 (9)	C(36)	11898 (21)	3229 (12)	8115 (16)	99 (10)
C(8)	−120 (19)	3817 (18)	1566 (12)	99 (11)	C(37)	11651 (19)	2971 (12)	8889 (14)	93 (10)
C(9)	574 (20)	4502 (15)	2280 (14)	102 (11)	C(38)	10345 (19)	2594 (12)	9035 (11)	80 (8)
C(10)	907 (16)	4159 (13)	3033 (10)	76 (8)	C(39)	7596 (15)	972 (11)	9019 (9)	66 (7)
C(11)	4652 (14)	3147 (13)	4707 (10)	94 (9)	C(40)	8286 (21)	351 (13)	8850 (14)	123 (12)
C(12)	3310 (17)	1546 (10)	3362 (11)	92 (9)	C(41)	8145 (22)	−538 (13)	9180 (15)	118 (12)
C(13)	3737 (16)	3581 (11)	3075 (10)	68 (8)	C(42)	7283 (20)	−850 (14)	9705 (11)	88 (9)
C(14)	3263 (16)	3284 (13)	2197 (11)	79 (8)	C(43)	6600 (22)	−257 (17)	9925 (17)	146 (15)
C(15)	3526 (19)	3974 (17)	1631 (12)	92 (10)	C(44)	6777 (19)	650 (15)	9594 (16)	130 (13)
C(16)	4266 (21)	4947 (17)	1910 (15)	107 (12)	C(45)	6631 (15)	1697 (11)	7698 (9)	63 (7)
C(17)	4761 (21)	5250 (14)	2757 (16)	116 (12)	C(46)	6457 (16)	872 (11)	7101 (10)	74 (8)
C(18)	4482 (18)	4572 (13)	3335 (12)	97 (9)	C(47)	5533 (18)	609 (12)	6341 (11)	85 (8)
C(19)	−1223 (17)	3475 (13)	5345 (10)	101 (10)	C(48)	4729 (19)	1134 (15)	6149 (13)	108 (11)
C(20)	−1881 (17)	1364 (12)	5032 (1)	96 (9)	C(49)	4852 (29)	1943 (18)	6724 (16)	193 (19)
C(21)	−2350 (16)	2425 (16)	3645 (10)	74 (8)	C(50)	5769 (26)	2206 (16)	7472 (14)	161 (15)
b. *cis*(*Cl*),*trans*(*P*)-$[\mathrm{TcCl_2(PMe_2Ph)_2(phen)}]\mathrm{BPh_4}$									
Tc	1088.0 (3)	2633.1 (2)	4231.2 (2)	30 (1)	C(23)	−2243 (4)	2604 (3)	3774 (2)	43 (2)
P(1)	3230.2 (10)	2711.1 (8)	3811.1 (7)	40 (1)	C(24)	−3027 (4)	1725 (4)	3256 (3)	58 (2)
P(2)	−1082.5 (11)	2539.7 (8)	4654.5 (6)	39 (1)	C(25)	−3766 (5)	1785 (5)	2520 (3)	81 (3)
Cl(1)	2201.7 (11)	4199.4 (8)	5061.0 (7)	55 (1)	C(26)	−3728 (6)	2699 (7)	2295 (3)	91 (4)
Cl(2)	1493.2 (11)	1614.6 (9)	5229.7 (6)	56 (1)	C(27)	−2972 (6)	3573 (5)	2793 (3)	80 (3)
N(1)	636 (3)	3321 (2)	3193 (2)	31 (1)	C(28)	−2227 (4)	3534 (4)	3538 (3)	57 (2)
N(2)	21 (3)	1366 (2)	3343 (2)	34 (1)	C(29)	7374 (4)	2798 (3)	9113 (2)	37 (2)
B	7691 (5)	1954 (3)	8484 (3)	38 (2)	C(30)	6181 (5)	2606 (3)	9422 (3)	64 (2)
C(1)	−83 (4)	2651 (3)	2515 (2)	35 (2)	C(31)	5896 (5)	3317 (3)	9934 (3)	71 (2)
C(2)	−411 (4)	1608 (3)	2593 (2)	35 (2)	C(32)	6804 (5)	4270 (3)	10157 (3)	62 (2)
C(3)	−296 (4)	377 (3)	3431 (3)	51 (2)	C(33)	7973 (5)	4502 (3)	9845 (3)	54 (2)
C(4)	−1024 (5)	−379 (3)	2795 (3)	69 (2)	C(34)	8244 (4)	3784 (3)	9340 (2)	45 (2)
C(5)	−1443 (5)	−145 (3)	2053 (3)	68 (2)	C(35)	9238 (4)	2415 (3)	8319 (2)	40 (2)
C(6)	−1146 (4)	873 (3)	1927 (2)	49 (2)	C(36)	9605 (5)	2617 (3)	7560 (3)	52 (2)
C(7)	−1559 (5)	1212 (4)	1176 (3)	63 (2)	C(37)	10925 (5)	2999 (4)	7438 (3)	68 (2)
C(8)	−1252 (5)	2203 (4)	1104 (3)	61 (2)	C(38)	11955 (5)	3194 (3)	8085 (4)	70 (2)
C(9)	−491 (4)	2963 (3)	1771 (2)	46 (2)	C(39)	11662 (5)	3015 (3)	8854 (3)	63 (2)
C(10)	−115 (5)	4008 (4)	1733 (3)	59 (2)	C(40)	10334 (4)	2639 (3)	8960 (3)	51 (2)
C(11)	631 (5)	4662 (3)	2400 (3)	59 (2)	C(41)	7497 (4)	863 (3)	8865 (2)	35 (2)
C(12)	998 (4)	4307 (3)	3121 (3)	44 (2)	C(42)	8476 (4)	404 (3)	8967 (3)	52 (2)
C(13)	4665 (4)	3107 (4)	4626 (3)	70 (2)	C(43)	8279 (5)	−522 (3)	9269 (3)	63 (2)
C(14)	3190 (5)	1487 (3)	3356 (3)	70 (2)	C(44)	7060 (5)	−1045 (3)	9477 (3)	55 (2)
C(15)	3684 (4)	3560 (3)	3045 (2)	41 (2)	C(45)	6054 (5)	−639 (3)	9370 (2)	52 (2)
C(16)	3185 (4)	3235 (3)	2220 (3)	55 (2)	C(46)	6272 (4)	283 (3)	9066 (2)	49 (2)
C(17)	3444 (5)	3932 (5)	1652 (3)	71 (3)	C(47)	6612 (4)	1690 (3)	7621 (2)	39 (2)
C(18)	4196 (6)	4916 (5)	1900 (4)	81 (3)	C(48)	6439 (4)	865 (3)	7059 (2)	49 (2)
C(19)	4695 (5)	5227 (4)	2706 (4)	77 (3)	C(49)	5519 (4)	594 (3)	6330 (2)	50 (2)
C(20)	4444 (5)	4564 (3)	3280 (3)	59 (2)	C(50)	4710 (5)	1144 (4)	6147 (3)	70 (2)
C(21)	−1091 (5)	3516 (3)	5448 (2)	59 (2)	C(51)	4834 (7)	1949 (5)	6688 (4)	126 (4)
C(22)	−1884 (5)	1372 (3)	5054 (3)	67 (2)	C(52)	5769 (6)	2231 (4)	7401 (3)	101 (3)
c. *cis*(*Cl*),*trans*(*P*)-$[\mathrm{TcCl_2(PEtPh_2)_2(bpy)}]\mathrm{SO_3CF_3}$									
Tc	904 (1)	2998 (1)	1948 (1)	19 (1)	C(7)	−1484 (8)	3364 (7)	625 (14)	60 (6)
Cl(1)	1179 (2)	3527 (1)	3733 (2)	36 (1)	C(8)	−1860 (9)	3749 (8)	1417 (18)	89 (8)
Cl(2)	2205 (2)	2565 (1)	1703 (2)	29 (1)	C(9)	−1458 (9)	3903 (7)	2452 (15)	76 (7)
P(1)	603 (1)	2062 (1)	3141 (2)	22 (1)	C(10)	−690 (7)	3679 (5)	2657 (11)	45 (5)
P(2)	1384 (2)	3869 (1)	681 (2)	27 (1)	C(11)	1417 (7)	1866 (5)	4185 (9)	34 (4)
N(1)	−314 (5)	3313 (4)	1830 (8)	32 (3)	C(12)	1268 (9)	1335 (7)	5030 (11)	63 (6)
N(2)	464 (5)	2582 (4)	358 (7)	23 (3)	C(13)	−296 (6)	2052 (5)	4084 (8)	24 (3)
C(1)	−735 (6)	3145 (5)	827 (11)	34 (4)	C(14)	−494 (9)	2580 (6)	4719 (9)	47 (5)
C(2)	−292 (7)	2733 (5)	14 (10)	37 (4)	C(15)	−1192 (7)	2584 (6)	5467 (10)	43 (5)
C(3)	892 (8)	2191 (4)	−325 (8)	29 (3)	C(16)	−1654 (7)	2080 (7)	5587 (10)	44 (5)
C(4)	555 (8)	1931 (6)	−1367 (9)	45 (4)	C(17)	−1455 (8)	1566 (6)	4995 (10)	45 (5)
C(5)	−206 (8)	2090 (7)	−1719 (11)	55 (5)	C(18)	−784 (7)	1552 (5)	4226 (9)	33 (4)
C(6)	−651 (9)	2504 (7)	−1041 (11)	54 (5)	C(19)	488 (6)	1412 (4)	2123 (8)	22 (3)

Table III (Continued)

atom	*x*	*y*	*z*	*U*(eq)[a]
C(20)	−245 (7)	1337 (5)	1510 (9)	32 (4)
C(21)	−346 (7)	887 (5)	683 (10)	40 (4)
C(22)	283 (9)	485 (6)	437 (11)	53 (5)
C(23)	1016 (9)	564 (6)	1008 (10)	49 (5)
C(24)	1120 (7)	1030 (5)	1849 (11)	43 (4)
C(25)	618 (8)	4472 (6)	534 (12)	56 (5)
C(26)	551 (9)	4861 (6)	1660 (13)	69 (6)
C(27)	1568 (7)	3596 (5)	−850 (9)	30 (4)
C(28)	2323 (9)	3320 (6)	−1083 (10)	44 (5)
C(29)	2455 (8)	3044 (8)	−2228 (10)	66 (6)
C(30)	1825 (11)	3099 (7)	−3086 (12)	74 (6)
C(31)	1106 (10)	3369 (7)	−2832 (11)	63 (6)
C(32)	968 (9)	3615 (5)	−1724 (9)	48 (5)
C(33)	2312 (7)	4281 (5)	1059 (9)	29 (4)
C(34)	2787 (7)	4135 (6)	2044 (11)	45 (4)
C(35)	3460 (9)	4473 (7)	2319 (10)	54 (5)
C(36)	3678 (8)	4974 (6)	1639 (12)	54 (5)
C(37)	3206 (9)	5119 (6)	675 (15)	63 (6)
C(38)	2546 (8)	4795 (5)	377 (12)	45 (5)
C(39)	6373 (14)	5129 (9)	2734 (20)	103 (10)
F(1)	7025 (9)	5003 (6)	3401 (14)	167 (8)
F(2)	6279 (9)	4597 (5)	2190 (13)	157 (7)
F(3)	5810 (15)	5110 (11)	3548 (19)	297 (15)
S	6327 (3)	5766 (2)	1946 (5)	76 (2)
O(1)	5630 (9)	5788 (6)	1293 (14)	132 (7)
O(2)	6609 (14)	6217 (6)	2553 (16)	200 (11)
O(3)	7022 (18)	5578 (15)	1088 (25)	340 (22)

[a] Equivalent isotropic *U* defined as one-third of the trace of the orthogonalized $\mathbf{U}_{ij}$ tensor.

Table IV. Selected Bond Lengths and Angles for *cis*(*Cl*),*trans*(*P*)-$[TcCl_2(PMe_2Ph)_2(bpy)]^+$ (A), *cis*(*Cl*),*trans*(*P*)-$[TcCl_2(PMe_2Ph)_2(phen)]^+$ (B), and *cis*(*Cl*),*trans*(*P*)-$[TcCl_2(PEtPh_2)_2(bpy)]^+$ (C)[a]

Bond Lengths (Å)

bond	A	B	C
Tc–Cl(1)	2.357 (4)	2.336 (1)	2.339 (3)
Tc–Cl(2)	2.357 (4)	2.371 (1)	2.350 (3)
Tc–P(1)	2.456 (5)	2.448 (1)	2.487 (3)
Tc–P(2)	2.477 (5)	2.474 (1)	2.496 (3)
Tc–N(1)	2.056 (11)	2.124 (3)	2.117 (8)
Tc–N(2)	2.059 (12)	2.094 (3)	2.113 (8)

Bond Angles (deg)

bond	A	B	C
P(2)–Tc–P(1)	179.3 (2)	179.6 (1)	172.3 (1)
Cl(1)–Tc–P(1)	87.9 (2)	88.2 (1)	89.7 (1)
Cl(1)–Tc–P(2)	92.0 (2)	92.2 (1)	92.2 (1)
Cl(2)–Tc–P(1)	87.7 (2)	88.6 (1)	84.9 (1)
Cl(2)–Tc–P(2)	91.5 (2)	91.2 (1)	87.5 (1)
Cl(2)–Tc–Cl(1)	95.0 (2)	97.0 (1)	96.6 (1)
N(1)–Tc–P(1)	89.8 (3)	89.3 (1)	96.5 (2)
N(1)–Tc–P(2)	91.0 (3)	90.9 (1)	90.8 (2)
N(1)–Tc–Cl(1)	95.0 (4)	92.7 (1)	94.2 (3)
N(1)–Tc–Cl(2)	169.6 (4)	170.4 (1)	168.7 (3)
N(2)–Tc–P(1)	92.6 (3)	92.2 (1)	91.3 (2)
N(2)–Tc–P(2)	87.5 (3)	87.5 (1)	88.0 (2)
N(2)–Tc–Cl(1)	171.7 (4)	170.8 (1)	170.6 (2)
N(2)–Tc–Cl(2)	93.3 (4)	92.6 (1)	92.3 (2)
N(2)–Tc–N(1)	76.7 (5)	78.2 (1)	76.5 (3)

[a] Numbers in parentheses are estimated errors in the final digit.

cis(*Cl*),*trans*(*P*)-$[TcCl_2(PMe_2Ph)_2(phen)]^+$, Figure 3; *cis*(*Cl*),*trans*(*P*)-$[TcCl_2(PEtPh_2)_2(bpy)]^+$, Figure 4. Additional plots viewed down the P–Tc–P axes are presented in Figure 5. Anisotropic temperature parameters (Table A), hydrogen atom coordinates (Table B), complete listings of bond lengths (Table C) and angles (Table D), observed and calculated structure factors (Table E), and structure plots for the counterions in each structure (Figure A) have been deposited as supplementary material.

Discussion

Synthesis and Characterization. New cationic technetium(III) complexes of the general formula *cis*(*Cl*),*trans*(*P*)-$[TcCl_2(P)_2L]^+$, where (P) is dimethylphenylphosphine or ethyldiphenylphosphine and L is 2,2′-bipyridine, 4,4′-dimethyl-2,2′-bipyridine, or 1,10-phenanthroline, have been synthesized and characterized. They are prepared by L substitution onto, with concomitant displacement of one chloride and one phosphine ligand from, the *mer*-trichlorotris(phosphine)technetium(III) starting material. This starting material is not stable over long periods in solution,[10] a fact that presumably facilitates its use in these reactions. The resulting bipyridyl complexes, for the most part, are stable in solution over at least several weeks, indicating that the coordination of the bipyridine and phenanthroline ligands stabilizes the Tc(III) center. The complexes are formed in a short period of time (approximately 30 min in refluxing ethanol), but the amount of product decreases if the reflux is allowed to proceed for longer periods. Chromatographic analysis of a reaction mixture that had been under reflux for 24 h shows that the amounts of the other byproducts are increased. The number of byproducts also appears to increase, as evidenced by an increase in the number of detectable chromatographic bands, rendering complete separation of the mixture impossible. Prolonged reflux, especially under a nitrogen blanket, also increases the yield of the Tc(II) analogue[14] (i.e., the second, green band in the chromatographic separation).

These complexes are particularly well suited to analysis by fast atom bombardment (FAB) mass spectrometry in the positive ion mode. Figure 1a shows the mass spectrum of $[TcCl_2(PMe_2Ph)_2(bpy)]^+$, which is typical for this class of complexes. The cluster of peaks at *m/e* 601 results from the molecular ion M^+ and exhibits an isotope distribution pattern that is consistent with a species containing two chlorine atoms. Additionally, the spectrum exhibits several other peaks that may be assigned as fragments of the complex resulting from the loss of monodentate ligands. That is, the doublet at *m/e* 566, 568 represents the molecular ion minus a chlorine, the triplet at *m/e* 463, 465, 467 represents loss of a phosphine ligand from the molecular ion, the peak at *m/e* 428 represents loss of one Cl and one phosphine, and that at *m/e* 393 is due to loss of two Cl and one phosphine ligand and so on. This fragmentation behavior results in a mass spectrometric "fingerprint", and observation of this "fingerprint" pattern for other analogues (see Figure 1) allows identification of these species. FAB mass spectra were also collected on chromatographic fractions other than the major product to allow reasonable assignments of the identities of some of these fractions. For example, the green fraction preceding the major fraction in the chromatography of the reaction mixtures exhibits a mass spectrum essentially the same as that of the major fraction, indicating that this band consists of the technetium(II) analogue of the major fraction. The Tc(II) oxidation state of these complexes is readily accessible both chemically and electrochemically.[14] The FAB mass spectra of these green products exhibit the same molecular ions and fragmentation patterns as do the Tc(III) complexes, indicating that the Tc(II) analogues are oxidized to the cationic Tc(III) species in the ion source. Other, later eluting, chromatographic fractions usually are not pure but give evidence for the existence of minor products, one of which as the general formula $TcCl(P)_3L$. These later fractions usually consist of small amounts of products and are poorly resolved.

UV–visible spectrophotometric parameters of these complexes, along with the parameters of the *mer*-$TcCl_3(PMe_2Ph)_3$ starting material, are given in Table II. The magnitude of the extinction coefficients in the visible region suggests that these absorptions are due to charge-transfer transitions, most likely metal-to-ligand charge transfers (MTLCT). The MTLCT phenomenon is well established for bipyridyl complexes of low-valent transition metals[3c] and is considered to result from metal $d\pi$ to ligand π^* transitions. The MTLCT band(s) in these complexes could in principle arise from two possible transitions: Tc to phosphine or Tc to bipyridine.

Table V. Selected Bond Distances for Related Tc(III), Re(III), and Ru(III) Complexes

complex	bond dist,^{a} Å			ref
	M–P	M–N	M–Cl, Br	
cis(*Cl*),*trans*(*P*)-$[TcCl_2(PMe_2Ph)_2(bpy)]^+$	2.467 (5)	2.058 (12)^b	2.357 (4)^c	*d*
cis(*Cl*),*trans*(*P*)-$[TcCl_2(PMe_2Ph)_2(phen)]^+$	2.461 (1)	2.109 (3)^b	2.354 (1)^c	*d*
cis(*Cl*),*trans*(*P*)-$[TcCl_2(PEtPh_2)_2(bpy)]^+$	2.492 (3)	2.115 (8)^b	2.345 (3)^c	*d*
trans(*Cl*)-$[Tc(DMPE)_2Cl_2]^+$	2.436 (5)		2.323 (4)	15
trans(*Cl*)-$[Tc(DPPE)_2Cl_2]^+$	2.501 (1)		2.319 (1)	16
trans(*Br*)-$[Tc(DPPE)_2Br_2]^+$	2.500 (1)		2.440 (1)	17
mer-$TcCl_3(PMe_2Ph)_3$	2.42 (1)		2.45 (1)^e 2.33 (1)^b	19
trans(*P*)-$[Tc(PPh_3)_2((acac)_2en)]^+$	2.51 (1)	2.06 (2)^f		18
$Tc(tmbt)_3(MeCN)_2$^{g}		2.042 (8)^c		24
$Tc(tmbt)_3(CO)(MeCN)$^{g}		2.166 (4)^h		24
$Tc(tmbt)_3(CO)(py)$^{g,i}		2.25 (2)^h		24
$TcL'(quin)PEt_2Ph$^{j}	2.41 (1)^c	2.15 (2)^e		20
$TcCl(phsal)_2(PMe_2Ph)$^{k}	2.412 (4)^c	2.126 (9)^b 2.132 (10)^e	2.427 (4)^c	21
cis(*Cl*),*trans*(*P*)-$ReCl_2(phsal)(PMe_2Ph)_2$^{k}	2.449 (1)	2.088 (7)	2.383 (3)^f 2.468 (2)^c	26
trans(*P*)-$ReCl_3(MeCN)(PPh_3)_2$	2.48 (12)	2.05 (3)	2.36 (1)^b	27
cis-$[Ru(bpy)_2Cl_2]^+$		2.050 (5)^b 2.060 (5)^c	2.325 (2)	25

[a] All bond distances listed are average values for like bonds. [b] Trans to Cl. [c] Trans to N. [d] This work. [e] Trans to P. [f] Trans to O. [g] tmbt = 2,3,5,6-tetramethylbenzenethiolate. [h] Trans to C. [i] py = pyridine. [j] quin = quinolin-8-olate, L′ = *N*-(2-oxidophenyl)salicylideneaminate. [k] phsal = *N*-phenylsalicylideneaminate.

However, the presence of visible absorption bands in these new complexes contrasts with the spectrum of the starting material wherein only a weak band at 481 nm and a moderate band at 381 nm appear, suggesting that the new, more intense absorptions are associated with the L ligand. The appearance of the bands in the range 535–540 nm strongly suggests that these bands are due to a metal–bpy (or phen) interaction as is the case for the rhenium analogue of $[TcCl_2(PMe_2Ph)_2(bpy)]^+$.[4] The Re species exhibits an absorption at 548 nm (ϵ = 2750 M^{-1} cm^{-1}) and like the Tc case, the starting material is relatively transparent in the visible region. The bands in the 360–388-nm range, as well as the band at 381 nm in the starting material, could be due to Tc–phosphine transitions. However, it might be expected that all of these transitions should be at higher energies relative to the corresponding transition in the starting material due to stabilization of the Tc dπ orbitals by π-back-bonding to the bpy ligand. Alternatively, since the molar extinction coefficients of these bands in the new complexes are greater than that of the starting material, the new bands could be a composite of Tc-to-P MTLCT and Tc-to-L MTLCT.

X-ray Crystal Structures. Complete crystal structure analyses of three analogous Tc(III) complexes present an opportunity to evaluate the structural effects resulting from small changes in ligands. All three complexes contain a technetium atom residing in a slightly distorted octahedral environment, with two trans phosphine ligands, and two cis chlorine atoms that are both *trans* to the two nitrogen atoms of the coordinating bidentate bpy or phen ligand. In the solid state, the complexes exhibit no mirror or axial symmetry, and therefore, the two phosphine ligands are not crystallographically equivalent. This is made even more apparent when the complexes are viewed down the P–Tc–P axes (Figure 5). Considering the two PMe_2Ph complexes (Figure 5a,b), the phenyl rings associated with P(1) in both cases are further removed from possible interactions with the bpy or phen rings than are the phenyl rings on P(2). In addition, Cl(1) in both cases eclipses a methyl carbon atom on P(2) (C(19) in Figures 2 and 5a for the bpy analogue and C(21) in Figures 3 and 5b for the phen analogue), whereas all methyl carbon atoms of P(1) are staggered with respect to the chlorine atoms. These facts together most likely account for the Tc–P(1) distances being slightly shorter (0.021–0.026 Å) than the Tc–P(2) distances in both cases (see Table IV). For the $PEtPh_2$ complex, the phenyl ring C(19)–C(24) of P(1) is in closest proximity to the bpy ligand and there are no atoms eclipsing the chlorine atoms (see Figure 5c); as a result, the Tc–P distances are more similar (0.009 Å difference) with Tc–P(1) being the shorter. Although the P(1)–Tc distance is 0.009 (3) Å shorter than the P(2)–Tc distance, the P(1) phosphine ligand is canted away from the bpy moiety more than is the P(2) phosphine ligand, as is evidenced by the average N(1,2)–Tc–P angles of 93.9 (2)° for P(1) and 89.4 (2)° for P(2) (difference = 4.5 (3)°). This effect is also observed in the PMe_2Ph complexes but to a lesser extent, with the difference in the N(av)–Tc–P angles being only 1.9 (3)° for the bpy analogue and 1.6 (2)° for the phen analogue. Table V lists selected bond distances for a variety of metal complexes with comparable ligands. The range of values of the Tc–P distances of the title complexes (2.448 (1)–2.496 (3) Å) falls within the range of values reported for Tc(III)–P distances in *trans*-$[Tc(DMPE)_2Cl_2]^+$,[15] *trans*-$[Tc(DPPE)_2Cl_2]^+$,[16] *trans*-$[Tc(DPPE)_2Br_2]^+$,[17] and *trans*-$[Tc(PPh_3)_2((acac)_2en)]^+$,[18] and the values are larger than the Tc(III)–P(trans-to-P) distances reported for the *mer*-$TcCl_3(PMe_2Ph)_3$ starting material.[19] The average Tc–P distances for *cis*(*Cl*),*trans*(*P*)-$[TcCl_2[PMe_2Ph)_2(bpy)]^+$, *cis*(*Cl*),*trans*(*P*)-$[TcCl_2(PMe_2Ph)_2(phen)]^+$, and *cis*-(*Cl*),*trans*(*P*)-$[TcCl_2(PEtPh_2)_2(bpy)]^+$, along with the other values mentioned above, show a trend in Tc–P bond distances where DMPE < PMe_2Ph < $PEtPh_2$ < DPPE = PPh_3. This trend seems reasonable since the bulkier ligands should exhibit longer distances because of steric interactions, and also because the more aromatic phosphine ligands are poorer σ donors, thus forming weaker bonds. The Tc–P distances are somewhat larger (ca. 0.05–0.08 Å larger than the Tc–P(trans-to-N) distances in two Tc/phosphine/Schiff base complexes[20,21] (Table V). They also compare well with Re–P distances observed in some Re(III) complexes containing trans phosphine ligands (Table V).

The Tc–N distances are more difficult to compare because the number of structure reports containing nitrogen bonded to Tc(III) is limited. However, the distances reported herein fall within the range noted for Tc–N distances in a variety of Tc complexes of different oxidation states and N donor ligands (2.001 (3)–2.259 (4) Å).[22,23] The only structures reported that contain Tc(III)–imine(N) distances are those of the Tc(III)–phosphine–Schiff base complexes *trans*-$[Tc(PPh_3)_2((acac)_2en)]^+$,[18] $TcL'(quin)(PEt_2Ph)$ (quin = quinolin-8-olate, L′ = *N*-(2-oxidophenyl)salicylideneaminate),[20] and $TcCl(phsal)_2(PMe_2Ph)$ (phsal = *N*-phenylsalicylideneaminate),[21] and also $Tc(tmbt)_3(CO)(py)$ (tmbt = 2,3,5,6-tetramethylbenzenethiolate, py = pyridine)[24] (see Table V). The Tc–N distance in *cis*(*Cl*),*trans*(*P*)-$[TcCl_2(PMe_2Ph)_2(bpy)]^+$ compares well with the Ru–N(trans-to-Cl) distances reported for *cis*-$[Ru(bpy)_2Cl_2]^+$[25] (Table V). The Tc–N distance in *trans*-$ReCl_2(phsal)(PMe_2Ph)_2$[26] falls within the range of values observed for the three complexes herein described. The range of Tc–N distances observed for the title complexes is in agreement with values given above; differences can be rationalized by steric arguments. Considering the two bpy complexes, the

---

(15) Vanderheyden, J.-L.; Ketring, A. R.; Libson, K.; et al. *Inorg. Chem.* **1984**, *23*, 3184.

(16) Libson, K.; Doyle, M. N.; Thomas, R. W.; et al. *Inorg. Chem.* **1988**, *27*, 3614.

(17) Libson, K.; Barnett, B. L.; Deutsch, E. *Inorg. Chem.* **1983**, *22*, 1695.

(18) Jurisson, S.; Dancey, K.; McPartlin, M.; Tasker, P. A.; Deutsch, E. *Inorg. Chem.* **1984**, *23*, 4743.

(19) Bandoli, G.; Clemente, D. A.; Mazzi, U.; Roncari, E. *J. Chem. Soc., Dalton Trans.* **1976**, 125.

(20) Mazzi, U.; Refosco, F.; Tisato, F.; Bandoli, G.; Nicolini, M. *J. Chem. Soc., Dalton Trans.* **1988**, 847.

(21) Duatti, A.; Marchi, A.; Luna, S. A.; Bandoli, G.; Mazzi, U.; Tisato, F. *J. Chem. Soc., Dalton Trans.* **1987**, 867.

(22) Melnik, M.; Van Lier, J. E. *Coord. Chem. Rev.* **1987**, *77*, 275.

(23) Bandoli, G.; Mazzi, U.; Roncari, E.; Deutsch, E. *Coord. Chem. Rev.* **1982**, *44*, 191.

(24) de Vries, N.; Dewan, J. C.; Jones, A. G.; Davison, A. *Inorg. Chem.* **1988**, *27*, 1574.

(25) Eggleston, D. S.; Goldberg, K. A.; Hodgson, D. J.; Meyer, T. J. *Inorg. Chem.* **1985**, *24*, 4573.

(26) Ferretti, V.; Sacerdoti, M.; Bertolasi, V.; Rossi, R. *Acta Crystallogr., Sect. C* **1984**, *C40*, 974.

analogue with $PEtPh_2$ has longer average Tc–N bond distances (2.115 (8) Å) than the analogue with PMe_2Ph (2.058 (12) Å) because of the greater steric bulk associated with the $PEtPh_2$ moiety. This steric crowding is also apparent when the P–Tc–P bond angles are considered: 172.3 (1)° for the $PEtPh_2$ complex and 179.3 (2)° for the PMe_2Ph complex, both with the phosphine groups being canted away from the bpy ligand. The Tc–N distances in the complex containing phen are on the average ca. 0.05 Å longer than those in the bpy complex (same phosphine included) and are due to the rigidity of the phen ligand and the larger bite angle required by this rigidity.

The Tc–Cl distances vary by only 0.035 Å among the three complexes reported here and are approximately equal to the Tc–Cl(trans-to-Cl) distances reported for the *mer*-$TcCl_3(PMe_2Ph)_3$ starting material.[19] However, they are much smaller than the Tc–Cl distance reported where the Cl is trans to a phosphine in the starting material. This suggests that the Cl atoms in the complexes reported herein are not subjected to as significant a structural trans effect (STE) from the imine nitrogen atoms as are the Cl atoms that are trans to phosphine moieties.[21] They are approximately 0.08 Å shorter than the Tc–Cl(trans-to-N) distance reported for $TcCl(phsal)_2(PMe_2Ph)$.[23] The Tc–Cl distances are, however, somewhat larger than the Tc–Cl(trans-to-Cl) distances reported for *trans*-$[Tc(DPPE)_2Cl_2]^+$[16] and *trans*-$[Tc(DMPE)_2Cl_2]^+$[15] where no STE is expected. They are also larger than the Ru–Cl(trans-to-bpy) distances reported for *cis*-$[Ru(bpy)_2Cl_2]^+$[25] owing to the higher effective nuclear charge on Ru(III). However, they are somewhat shorter than the Re–Cl(trans-to-MeCN) distance observed for *trans*(*P*)-$ReCl_3(MeCN)(PPh_3)_2$.[27]

Acknowledgment. Financial support by the National Institutes of Health, Grant No. CA-42179 (E.D.), as well as the University of Cincinnati Department of Chemistry, University Research Council, and University Dean's Distinguished Dissertation fellowship programs (B.E.W.), is gratefully acknowledged.

Registry No. A, 119818-89-2; B, 119818-91-6; C, 119818-93-8; $[TcCl_2(PMe_2Ph)_2(bpy)]PF_6$, 119818-94-9; *mer*-$TcCl_3(PMe_2Ph)_3$, 53749-02-3; *cis*(*Cl*),*trans*(*P*)-$[TcCl_2(PMe_2Ph)_2(Me_2bpy)]^+$, 119818-95-0; *cis*(*Br*),*trans*(*P*)-$[TcBr_2(PMe_2Ph)_2(bpy)]^+$, 119818-96-1; $[TcCl_2(PMe_2Ph)_2(bpy)]$, 119818-97-2; *mer*-$TcBr_3(PMe_2Ph)_3$, 53749-03-4; *mer*-$TcCl_3(PEtPh_2)_3$, 65013-98-1.

Supplementary Material Available: Tables of anisotropic temperature parameters (Table A), hydrogen atom coordinates (Table B), and complete bond lengths (Table C) and bond angles (Table D) and structure plots for the counterions (Figure A) for *cis*(*Cl*),*trans*(*P*)-$[TcCl_2(PMe_2Ph)_2(bpy)]BPh_4$, *cis*(*Cl*),*trans*(*P*)-$[TcCl_2(PMe_2Ph)_2(phen)]BPh_4$, and *cis*(*Cl*),*trans*(*P*)-$[TcCl_2(PEtPh_2)_2(bpy)]SO_3CF_3$ (14 pages); a listing of observed and calculated structure factors (Table E) (40 pages). Ordering information is given on any current masthead page.

---

(27) Drew, M. G. B.; Tisley, D. G.; Walton, R. A. *Chem. Commun.* **1970**, 600.

Notes

Contribution from the Department of Chemistry
and Ames Laboratory, Iowa State University,
Ames, Iowa 50011

2,3-Dihydrothiophene (2,3-DHT) Complexes of Tungsten. Structure of $W(CO)_3(dppe)(2,3\text{-}DHT)$

George N. Glavee, Lee M. Daniels, and Robert J. Angelici*

Received August 30, 1988

Catalytic hydrodesulfurization (HDS) is the process that removes sulfur from thiophene and other sulfur-containing organic compounds in crude oil. Model organometallic complexes of thiophene and thiophene derivatives have been studied in our research group in an effort to elucidate the mechanism of the HDS process.[1] The formation of 2,3-dihydrothiophene (2,3-DHT) has been proposed as the first step in the HDS of thiophene.[2] In an effort to examine the coordination modes of this partly hydrogenated thiophene, which potentially could coordinate through the olefin or the sulfur on the catalyst surface, a number of its transition-metal complexes have been prepared in recent years: $Mn(CO)_3Cl(2,3\text{-}DHT)$,[1a] $W(CO)_5(2,3\text{-}DHT)$,[3] $[Re(CO)_5(2,3\text{-}DHT)]SO_3CF_3$,[3] $Ru(CO)_3Cl_2(2,3\text{-}DHT)$,[3] and $PdCl_2(2,3\text{-}DHT)_2$.[3] We report in this paper the syntheses of a variety of phosphine-substituted tungsten complexes and the first X-ray-determined structure of a 2,3-DHT compound.

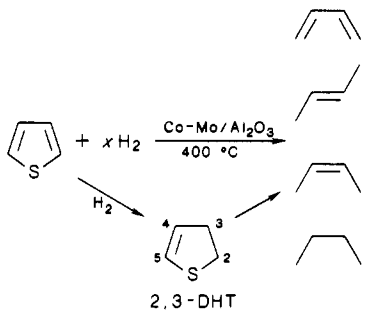

Experimental Section

General Procedures. All reactions were carried out under an atmosphere of prepurified N_2 at room temperature by using standard inert-atmosphere and Schlenk[4] techniques unless otherwise stated. Tetrahydrofuran (THF) and Et_2O were distilled under N_2 from Na/benzophenone. Pentane, hexane, MeCN, and CH_2Cl_2 were distilled from CaH_2 under N_2. Trimethylphosphine was prepared by the reaction of methyl Grignard reagent and triphenyl phosphite.[5]

Infrared spectra were obtained by using a Perkin-Elmer 681 spectrophotometer, and spectra were referenced to the 1944.0-cm^{-1} band of polystyrene. The ^1H data were recorded on a Nicolet NT-300 300-MHz spectrometer using Me_4Si as the internal reference. Low-temperature ^1H NMR spectra were obtained on a Bruker WM 300 300-MHz instrument. Electron impact mass spectra (EIMS) were obtained on a Finnigan 4000 instrument. Fast atom bombardment (FAB, glycerol matrix) mass spectra were obtained by using a Kratos MS-50 spectrometer. Photochemical reactions were carried out in a quartz Schlenk tube equipped with a cooling probe by using a reactor obtained from Bradford Scientific, Inc., Marblehead, MA.

---

(1) (a) Lesch, D. A.; Richardson, J. W., Jr.; Jacobson, R. A.; Angelici, R. J. *J. Am. Chem. Soc.* **1984**, *106*, 2901. (b) Huckett, S. C.; Sauer, N. N.; Angelici, R. J. *Organometallics* **1987**, *6*, 591. (c) Spies, G. H.; Angelici, R. J. *J. Am. Chem. Soc.* **1985**, *107*, 5569. (d) Sauer, N. N.; Angelici, R. J. *Organometallics* **1987**, *6*, 1146. (e) Spies, G. H.; Angelici, R. J. *Organometallics* **1987**, *6*, 1897. (f) Hachgenei, J. W.; Angelici, R. J. *Angew. Chem., Int. Ed. Engl.* **1987**, *26*, 909. (g) Hachgenei, J. W.; Angelici, R. J. *Organometallics* **1989**, *8*, 14. (h) Hachgenei, J. W.; Angelici, R. J. *J. Organomet. Chem.* **1988**, *355*, 359.

(2) (a) Angelici, R. J. *Acc. Chem. Res.* **1988**, *21*, 387. (b) Markel, E. J.; Schrader, G. L.; Sauer, N. N.; Angelici, R. J. *J. Catal.*, in press. (c) Devanneaux, J.; Maurin, J. *J. Catal.* **1981**, *69*, 202. (d) Zdrazil, M. *Collect. Czech. Chem. Commun.* **1975**, *40*, 3491. (e) Desikan, P.; Amberg, C. H. *Can. J. Chem.* **1964**, *42*, 843.

(3) Sauer, N. N.; Angelici, R. J. *Inorg. Chem.* **1987**, *26*, 2126.

(4) (a) Shriver, D. F.; Drezdon, M. A. *The Manipulation of Air Sensitive Compounds*, 2nd ed.; Wiley: 1986. (b) Herzog, S.; Dehnert, J.; Luhder, K. *Technique of Inorganic Chemistry*; Jonassen, H. B., Ed.; Interscience: New York, 1969; Vol. VII.

(5) Gibson, V. C.; Graimann, C. E.; Hare, P. M.; Green, M. L. H. *J. Chem. Soc., Dalton Trans.* **1985**, 2025.

0020-1669/89/1328-1751$01.50/0 © 1989 American Chemical Society